Effect of CO_2 Concentration on $YBa_2Cu_3O_{6+x}$ Formation

T. Kohav, K. M. Forster, J. T. Richardson, and D. Luss
Dept. of Chemical Engineering, University of Houston, Houston, TX 77204

Two reversible reactions are involved in $YBa_2Cu_3O_{6+x}$ formation: a reaction between $BaCO_3$ and CuO forming $BaCuO_2$ and CO_2, and a reaction of $BaCuO_2$ with Y_2O_3 and CuO forming $YBa_2Cu_3O_6$ which undergoes phase transformation to $YBa_2Cu_3O_{6+x}$ upon cooling. In-situ isothermal time resolved HT-XRD of a thin film was used to quantify the effect of CO_2 on the kinetics of the first reaction. Increased CO_2 partial pressure shifts the reactions to higher temperatures. At high CO_2 partial pressure (>2 vol. %), the rate of the first reaction becomes essentially a step process with a very high activation energy. Noninstantaneous nucleation of the reaction products occurs at low CO_2 partial pressure (0.5–1%) and temperatures (700°C). The data fit a 2-D diffusion-controlled mechanism with a zero nucleation rate for $BaCO_3$ decomposition and a second-order nucleation rate for $YBa_2Cu_3O_6$ formation. A comparison of the kinetics of a thin film (10 μm) as determined by HT-XRD with those of a thick sample (2 mm) determined by TG revealed that the transport of CO_2 within the sample pores and to the ambient gas significantly affect the decomposition of $BaCO_3$. For example, the formation of $YBa_2Cu_3O_6$ in a thick precursor layer occurs in the 840 to 940°C range, exceeding by about 200°C that in which it is formed in thin films.

Introduction

Solid-state reactions are involved in the synthesis of many important products such as metallurgical solutions, ceramics, cements, catalysts, fertilizers, drugs, and organic pigments. Knowledge of the kinetics of these reactions is essential for understanding their mechanism, improving product properties and purity, and reactor design and scale-up. Solid-state kinetic data are conventionally measured either by thermogravimetry (TG), differential thermal analysis (DTA), differential scanning calorimetry (DSC) or by the "quench and analyze" XRD technique in which separate samples are heated in a furnace in a specified sequence, and then quenched and analyzed by X-ray diffraction. High-temperature X-ray diffraction (HT-XRD) provides *in-situ* qualitative and quantitative information on the identity and quantity of all the crystalline chemical components and solid phases in the sample. In general, HT-XRD provides a more detailed and accurate description of solid-phase reactions. For example, Gerard's (1974) study of tungsten oxide reduction in hydrogen using TG suggested an apparent single-stage reduction. However, HT-XRD measurements revealed a considerably more complex reaction network involving three intermediates. Fawcett et al.'s (1985) HT-XRD study of the fusion of polyethylene showed that the process is much more intricate than that suggested by DSC measurements. The main obstacle in the past in the use of HT-XRD in kinetic studies was the requirement of fast data acquisition. This obstacle has been overcome by the advent of fast detection systems such as position sensitive detectors (Gabriel, 1977). Thus, the use of HT-XRD in kinetics studies of solid-state reactions is increasing (Nix et al., 1987; Thomson et al., 1988; Walker et al., 1989; Forster et al., 1994).

Several investigators have studied the rate of formation of $YBa_2Cu_3O_{6+x}$ high temperature superconductors. The conventional kinetic investigations of $YBa_2Cu_3O_{6+x}$ formation from mixed oxides were performed by Ruckenstein et al. (1989), Gadalla and Hegg (1989), Wu et al. (1990), and Sinha et al. (1993) using TG and the "quench and analyze" XRD. HT-XRD investigations of the reaction pathways and kinetics of $YBa_2Cu_3O_{6+x}$ formation from a spray roasted precursor

Correspondence concerning this article should be addressed to either J. T. Richardson or D. Luss.

of $BaCO_3$, Y_2O_3 and CuO were performed by Thomson et al. (1989), Shie and Thomson (1992), Formica et al. (1992), Forster et al. (1992), and Milonopoulou et al. (1994). These investigations were conducted either in inert or in oxidizing atmospheres. These studies show that two main reactions are involved in $YBa_2Cu_3O_{6+x}$ formation in oxidizing atmospheres

$$BaCO_{3(s)} + CuO_{(s)} \Leftrightarrow BaCuO_{2(s)} + CO_{2(g)}, \quad (1)$$

and

$$4BaCuO_{2(s)} + 2CuO_{(s)} + Y_2O_{3(s)} \Leftrightarrow 2YBa_2Cu_3O_{6(s)} + 0.5O_{2(g)}. \quad (2)$$

Poeppel et al. (1990) and Balachandran et al. (1991) found that vacuum processing of a mixed oxide precursor under controlled total oxygen pressure resulted in $YBa_2Cu_3O_{6+x}$ formation at 800°C, while at atmospheric pressure, the same reaction occurred at temperatures exceeding 800°C. Grader et al. (1989) found that vacuum processing of finely ground mixed-oxide precursor caused the first reaction to be almost complete at 550–600°C, while in air the reaction occurred at temperatures higher by more than 150°C. These results indicate that CO_2 removal by the vacuum accelerates the reaction. Sundaresan (1992) studied $YBa_2Cu_3O_{6+x}$ formation from a spray roasted precursor containing $BaCO_3$, Y_2O_3, and CuO. He showed that in thick samples 123 phase formed first in the exterior layer of the sample in both N_2 and O_2 environments. Subsequently, the product front propagated into the specimen. His study indicates that the rate of CO_2 removal from the interior of the sample significantly affects the progress of the reaction.

We report here a study on the influence of CO_2 concentration in air on the intrinsic kinetics of the $BaCO_3$ reaction with CuO and $YBa_2Cu_3O_6$ formation in thin sprayed samples by *in-situ* time resolved HT-XRD. These measurements are compared with the kinetics of thick samples, determined by isothermal TG experiments. The comparison and data about the influence of sample size and gas velocity provide useful information on the impact on the inter- and intrasample diffusional limitations of the evolved carbon dioxide on the observed reaction rate.

Experimental System

In-situ HT-XRD measurements were conducted using a Siemens D-5000 diffractometer in a vertical $\theta/2\theta$ configuration, which are equipped with a Bühler HDK 2.3 high temperature (hot) stage and a Braun position sensitive detector (PSD). Radiation from a fine focus 1.5 kW sealed-tube source with a Cu anode was focused by a Ge [111] incident beam monochromator yielding $K\alpha_1$ radiation. The PSD was configured to collect intensities over 5.26° 2θ at a rate which is two orders of magnitude faster than a scintillation detector. The intensities collected by the PSD were sorted by angle into a multichannel analyzer (MCA) and were later transferred to a host Micro VAX II computer.

The powder samples were sprayed onto a gold plated 90% platinum/10% rhodium strip [0.009 in. (0.23 mm) thick], which had been electroplated with a 0.5-μm-thick gold layer on the central 1.0–1.5 cm part of the strip (Dixie Electro Plating Inc.) to prevent the formation of barium-platinum-oxides at high temperatures. The sample strip was surrounded by a nearly cylindrical platinum/rhodium heater, roughly 30 mm in diameter, from which the upper 30° arc is removed to allow passage of the X-ray beam, while minimizing any thermal gradients near the sample. The sample temperature was monitored by an S-type thermocouple (Pt-Pt 10% Rh), spot-welded to the underside of the heating strip.

The thermogravimetric experiments were carried out in a Seiko simultaneous thermogravimetric differential thermal analyzer model TG/DTA320. The sample and reference materials were placed in 50μL, Platinum crucibles, mounted on Platinum/Rhodium sample holders in the front side of the two balances beams.

The powder used in this study was $YBa_2Cu_3O_{6+x}$ spray roasted precursor containing $BaCO_3$, Y_2O_3, and CuO manufactured by Seattle Specialty Ceramics, Inc. (SSC). The solid and particle densities are 4.2 and 2.9 g/cm^3, respectively. Detailed characterizations of these powders were reported by Shelukar (1993) and Shelukar et al. (1994). ICP measurements showed that the precursor powder contained $BaCO_3$, CuO and Y_2O_3 in the proper stoichiometric ratio to form 123. Thus, the initial mass fraction of $BaCO_3$ in the precursor powder is 0.53.

Experimental Procedure and Data Analysis

In-situ time-resolved HT-XRD

Standard X-ray powder diffraction analysis is done on samples sufficiently thick to either diffract or absorb the entire incident beam. Use of thin samples is preferred in high temperature X-ray diffraction (HT-XRD) kinetic studies to minimize the thermal gradients in the heated sample. Uniform, thin coatings of precursor powder on the heating strip were prepared by spraying a solution of suspended precursor in absolute ethanol with an artist's airbrush, and allowing the ethanol to evaporate. The effective sample thickness was determined prior to each high temperature scan by a procedure described by Forster et al. (1994). The sample temperature was calibrated using the thermal expansion of MgO following the procedure reported by Forster et al. (1994).

Prior to all high temperature experiments, the hot stage was flushed with the desired gases (N_2, O_2, CO_2) for at least 3 h. Next, a preliminary continuous scan of angular range $20° < 2\theta < 50°$, 0.02° resolution and a scan velocity of 0.5°/min was used to check sample purity and to measure sample thickness. Each high temperature experiment started with a 60 s fixed scan, 0.05° resolution at 30°C. In the experiments which followed the $BaCO_3$ decomposition, the intensities of the [111] and [021] reflections were followed in the 22.5° to 27.5° 2θ range.

The time dependence of the $BaCO_3$ mass fraction was determined from the ratio of the integrated intensity (peak areas) of the [111] and [021] reflections at time t and time = 0. CO_2 evolution by the decomposition reaction (Eq. 1) leads to a 12.9% sample weight loss upon complete conversion. The weight fraction at time t, $w(t)$ is computed by the relation

$$w(t) = \frac{[I_{[111]}(t) + I_{[021]}(t)]}{[I_{[111]}(0) + I_{[021]}(0)]\left[1 - 0.129^*\left(1 - \frac{w(t)}{w(0)}\right)\right]} w(0). \quad (3)$$

Any absorption corrections that may apply in this case essentially cancel, as the angular separation between the two reflections is small and the sample is very thin. The Rietveld refinement showed that there was no preferred orientation.

After heating at 1.5°C/s to 100°C and holding for 5 min, the sample was heated to the desired temperature at the rate of 10°C/s. Up to 60 multiple high temperature fixed scans (60 s long, 0.05° resolution) were performed at the set temperature. The opening and closing of the X-ray tube shutter resulted in a 2 s delay between scans. Following this, the sample was quenched at 20°C/s, and a final 60 s fixed scan was taken at 30°C. High temperature isothermal experiments following the 123 peaks were performed in the 28.5° to 33.5° 2θ range. This angular range includes the following reflections: the [103] and [110] of $YBa_2Cu_3O_6$; the [600] and [611] of $BaCuO_2$ and the [211], [204], and [013] and $Y_2Cu_2O_5$. After heating at 1.5°C/s to 100°C and holding for 5 min, the sample was heated to the desired temperature at 10°C/s and up to 50 multiple high temperature fixed scans (60 s long, 0.05° resolution) were performed. The first 30 successive fixed scans were taken with only a 2 s delay between scans to capture the initial stages of the reaction. The remaining scans were taken every 3 min. The sample was then quenched at 20°C/s and a final 60 s fixed scan was taken at 30°C. At the conclusion of the *in-situ* experiment, a continuous slow scan of the angular range $20° < 2\theta < 70°$ at 0.02° resolution was taken with a scan velocity of 0.3°/min for the $BaCO_3$ experiments and 0.2°/min for the $YBa_2Cu_3O_6$ experiments. The final room temperature scan in the experiments was used for quantitative analysis of the reaction products. The final mass fraction was calculated by a Rietveld refinement of the room temperature scan using the General Structural Analysis System (GSAS) developed at Los Alamos.

The time dependence of the $YBa_2Cu_3O_{6+x}$ mass fraction was determined from the ratio of the integrated intensity of the [103] and [110] reflections at time t, and $t = t_f$ where t_f corresponds to the final (room temperature) scan following the procedure described by Forster et al. (1994). Preliminary experiments showed that all the $BaCO_3$ has decomposed when the conversion to 123 exceeds 70%. The total weight loss associated with the reaction is about 12.9%. Approximating this weight loss to be linear with $w(t)/w(t_f)$, the mass fraction of 123 at time satisfies the relation

$$w(t) = \frac{[I_{[103]}(t) + I_{[110]}(t)](1 - 0.129)}{[I_{[103]}(t_f) + I_{[110]}(t_f)]\left[1 - 0.129^*\frac{w(t)}{w(t_f)}\right]} w(t_f). \quad (4)$$

The film thickness was determined by comparing the integrated intensities of the [111] and [021] of $BaCO_3$ with those of an infinitely thick sample. Reproducible results were obtained from films having μt in the range of (0.06–0.08), where μ is the linear absorption coefficient ($\sim 10^3$ cm^{-1}). This yields an effective thickness t of about 0.6–0.8 μm. The effective thickness was just an indication that the counting statistics were adequate and that the thermal gradients across the sample were minimal. Measurements under these conditions yielded reproducible results. Inspection of the film by a microprobe showed that it was essentially a single particle layer with a thickness less than 10 μm.

Isothermal TG kinetic study

TG experiments were usually conducted with 20 mg samples, which were purged with the gas mixture at flow rates of 500 cm^3/min for 2 h. The samples were then heated rapidly (5–6 min) to a set temperature and their weight was measured and recorded every second for 40 min to 4 h, depending on the rate of the weight loss. At the end of the experiment, the sample was cooled to room temperature at the rate of 40°C/min. Sample masses were 20 mg, with the exception of the experiments, to check the impact of sample size and gas velocity. Al_2O_3 was used as the reference material. A special set of experiments was conducted to determine the impact of the sample size and gas-flow rate. When the powder weight was less than 20 mg, the sample was placed on top of a Al_2O_3 bed so that the total weight of the powder and Al_2O_3 was 20 mg.

The raw TG weight loss data was corrected for base line loss that occurs before the reaction starts due to several effects such as: drift of the balance reading at high temperature, desorption of water, and so on. The correction was done by subtracting the weight loss obtained in the case of no reaction (that is, at sufficiently high CO_2 concentration) from that obtained at lower CO_2 concentration and the same temperature. Final conversions were calculated by dividing the overall weight loss percent of the corrected data by the maximum possible weight loss of 12.9%.

The TG temperature was calibrated by heating K_2CrO_4 at 5°C/min and comparing the temperature at which the endothermic peak of the α-to-β phase-transformation occurred to reported values (Garn and Menis, 1971). The weight loss was calibrated by heating of calcium oxalate $CaC_2O_4 \cdot H_2O$ at temperatures from 20–1,000°C at the rate of 40°C/min and comparing the weight loss to reported values (Seiko Operation Manual, 1989).

Experimental Results

XRD studies of thin films

The $BaCO_3$ decomposition reaction in thin films (10 μm) of $YBa_2Cu_3O_6$ precursor powder was studied in air mixtures containing 0.5, 1 and 2% carbon dioxide at several temperatures in the range of 645 to 765°C. Figure 1a describes a typical time dependence of the X-ray diffraction patterns. Raising the temperature increases the decomposition rate, while increasing the carbon dioxide concentration shifts the reaction to higher temperatures (Figure 2) and decreases the range of temperatures over which the reaction rate changes from negligible to essentially instantaneous within the experimental resolution of 60 s. For example, the range of temperatures corresponding to carbon dioxide concentrations of 0.5, 1.0, and 2.0 vol. % are 65, 55 and 35°C, respectively. An induction period of 25 to 15 min exists at a temperature range between 645 and 655°C for a mixture of 0.5 vol. % CO_2. A

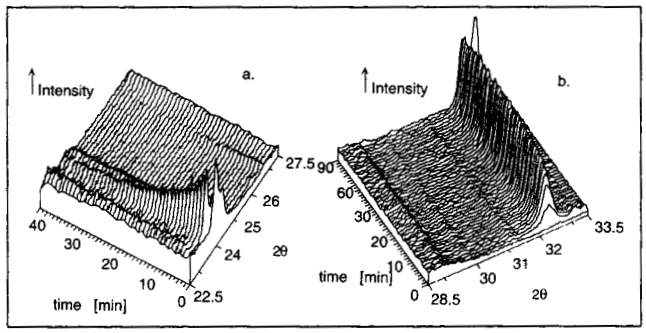

Figure 1. Multiple high-temperature scans of isothermal experiments following the $BaCO_3$ [111] and [021] peaks (705°C,a) and the $YBa_2Cu_3O_6$ [103] and [110] peaks (715°C, b) in air containing 1 vol. % CO_2.

four minute induction period exists at 685°C for a mixture containing 1 vol. % CO_2. An induction period was not observed for any experiment conducted at a temperature exceeding 685°C. Increasing the CO_2 concentration reduced the temperature range in which an induction was observed.

The $YBa_2Cu_3O_6$ formation kinetics was studied for mixtures containing 0.5, 1, and 2 vol. % CO_2 in air at several temperatures in the range of 680 to 755°C. A typical time dependence of the X-ray patterns in the range of 28.5–33.5° 2Θ (Figure 1b) shows a gradual increase in the intensity of the tetragonal $YBa_2Cu_3O_6$ [103] and [110] peaks, and the appearances of traces of $Y_2Cu_2O_5$ and $BaCuO_2$ peaks. As in the $BaCO_3$ decomposition, raising the temperature increases the reaction rate, while increasing the carbon dioxide concentration requires use of higher temperatures to maintain the same yield of the desired product (Figure 3). In all the experiments, the final yield of $YBa_2Cu_3O_6$ exceeded 73%. Repeated experiments for $YBa_2Cu_3O_6$ production led to less

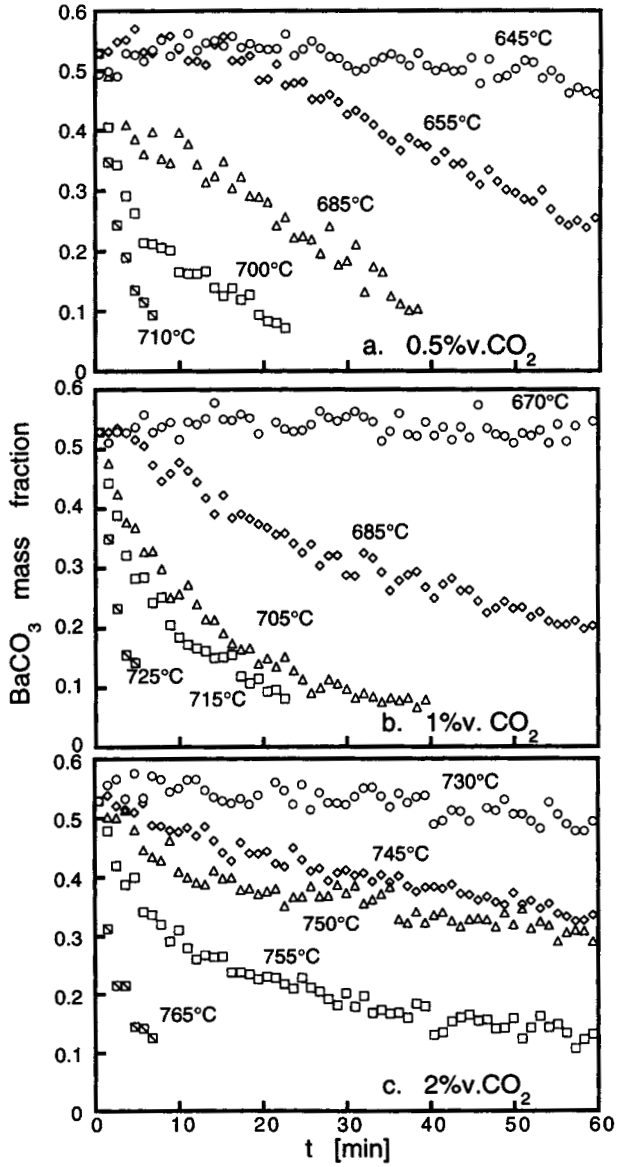

Figure 2. Kinetics of $BaCO_3$ decomposition in air containing (a) 0.5 vol. %; (b) 1 vol. %; and (c) 2 vol. % CO_2.

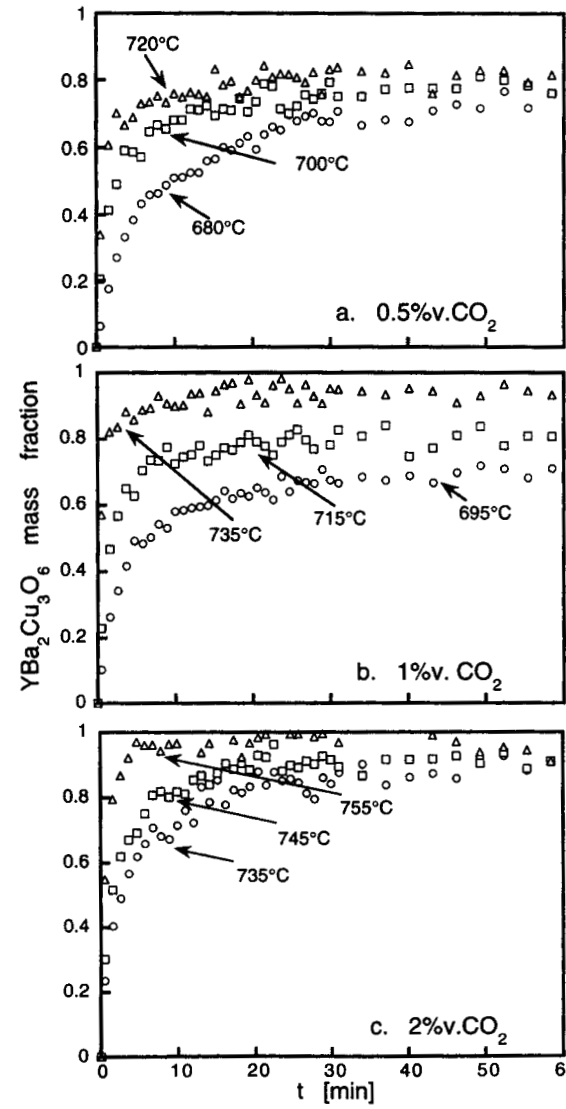

Figure 3. Kinetics of $YBa_2Cu_3O_6$ formation in air containing (a) 0.5 vol. %; (b) 1 vol. %; and (c) 2 vol. % CO_2 partial pressure in air.

Table 1. Values of the Kinetic Parameters Used in Eqs. 1 and 2

	$BaCO_3$ Decomposition				$YBa_2Cu_3O_{7-x}$ Formation			
CO_2, vol. %	T (K)	k_1 (min^{-1})	n	k_2 (min^{-1})	T (K)	k_3 (min^{-1})	k_4	w_e
0.5	655°C	0.006	1.27	0.018	680°C	0.69	1.00	0.76
0.5	685°C	0.046	0.92	0.035	700°C	2.19	1.05	0.77
0.5	700°C	0.221	0.69	0.108	720°C	4.28	1.16	0.80
1%	685°C	0.042	0.78	0.019	695°C	1.41	0.87	0.73
1%	705°C	0.106	0.82	0.064	715°C	3.16	0.90	0.83
1%	715°C	0.159	0.79	0.096	735°C	10.49	0.94	0.95
2%	745°C	0.014	0.87	0.008	735°C	1.63	1.01	0.89
2%	750°C	0.060	0.55	0.011	745°C	1.69	1.64	0.87
2%	755°C	0.155	0.55	0.034	755°C	3.45	2.20	0.95

than 2% variation. The main experimental error is due to the uncertainty in the value of the sample temperature, which was determined from high temperature calibrations with MgO. On the same strip and film, up to ±1°C differences may exist between two identical experiments. However, using different strips and films may increase this uncertainty to ±5°C.

The rate of the $BaCO_3$ decomposition fits very well a diffusion controlled nucleation and growth mechanism of the form (Hulbert, 1969)

$$w = w_o \exp[-k(t - t_o)^n] \tag{5}$$

where w and w_o are the instantaneous and initial weight of the reactant, and t_o is the induction time. Except for three experiments (0.5 vol. % CO_2 at 645 and 655°C, and 1 vol. % CO_2 at 685°C), the data fit closely a model with a zero induction time. The values of n and k (reported as k_1) which give the best fit are listed in Table 1. The value of n varies between 0.55 to 1.23 suggesting, according to Hulbert (1969), a one-dimensional diffusion controlled growth geometry (rods of the $BaCuO_2$ product) with a decreasing nucleation rate. Figure 4a describes the fit of the data at 1 vol. % CO_2 and various temperatures. The best fit of n for the temperatures of 685, 705 and 715°C were 0.78, 0.82, and 0.79, respectively. The data for most experiments could be fit adequately by assuming that $n = 1$, which corresponds to a two-dimensional diffusion controlled growth (plates) of the product with a zero-nucleation rate (that is, all nucleation sites are present initially). The data fit using $n = 1$ is shown in Figure 4b. Comparison of Figures 4a and 4b shows that imposing the value of $n = 1$ has only a minor impact on the quality of the fit. The corresponding rate constants are reported as k_2 in Table 1. The fit with $n = 1$ was not as good ($R = 0.83$) at 750°C and 755°C with 2 vol. % CO_2, that is, at the highest temperatures and CO_2 concentration. The poor fit under these conditions may be due to a change in the dimensionality of the product as the operating conditions are changed. A much better fit of these data ($R > 0.96$) is obtained for $n = 0.55$.

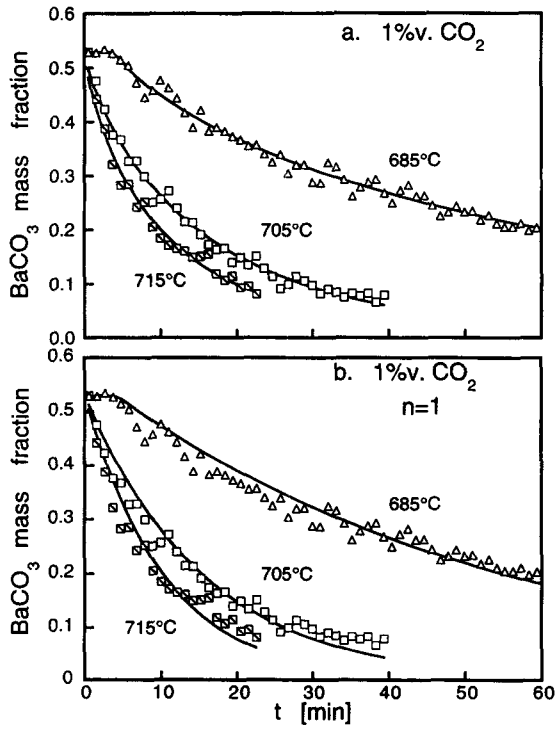

Figure 4. Nucleation and growth mechanism (Eq. 5) used to fit data of $BaCO_3$ decomposition in air containing 1 vol. % CO_2 partial pressure in air.

(a) With least-squares fit of n (= 0.78, 0.82 and 0.79 for 685, 705 and 715°C, respectively); (b) with $n = 1$.

The rate constants k_2 fit an Arrhenius temperature dependence. The corresponding pre-exponential factors and activation energies are listed in Table 2. The activation energies (range of 280–1,230 kJ/mol) are much higher than those of common chemical reactions. The drastic increase in the activation energies with CO_2 partial pressure is responsible for the shrinking of the temperature range over which the reaction rate changes from negligible to almost instantaneous.

Milonopoulou et al. (1994) have shown that the rate of $YBa_2Cu_3O_6$ formation in air can be fit well by a two-dimensional diffusion-controlled nucleation and growth mechanism (plate geometry) with a second-order nucleation rate, that is

Table 2. Values of the Preexponential Factor and Activation Energies of k_2, k_3 and k_4

CO_2 vol. %	log k_{02} (min^{-1})	E_{k2} (kJ/mol)	log k_{03} (min^{-1})	E_{k3} (kJ/mol)	log k_{04}	E_{k4} (kJ/mol)
0.5%	15	280	20	360	1.5	30
1%	20	430	20	410	0.75	15
2%	60	1,230	15	320	15	330

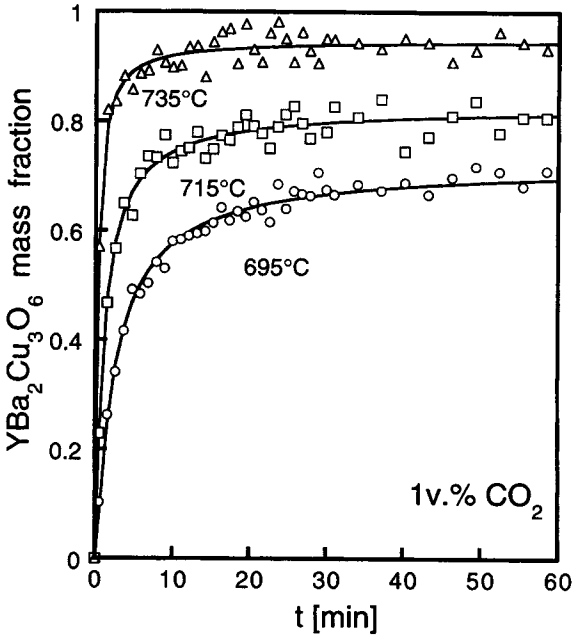

Figure 5. Nucleation and growth mechanism (Eq. 6) used to fit data of $YBa_2Cu_3O_6$ formation curves in air containing 1% CO_2.

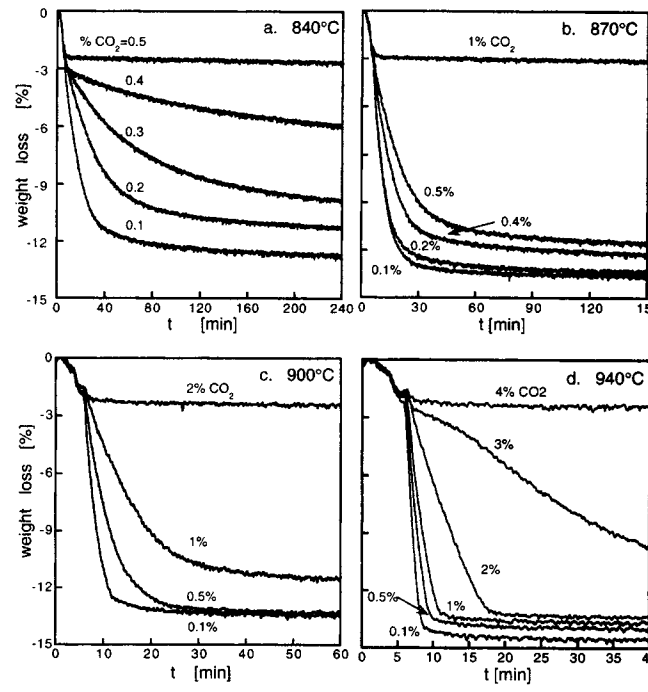

Figure 6. Effect of CO_2 partial pressure in air on the TG weight-loss at four temperatures.

$$1-\frac{w}{w_e}=\exp\left(\frac{k_3k_4t}{1+k_3t}\right)/(1+k_3t)^{k_4} \qquad (6)$$

where w and w_e are the instantaneous and final $YBa_2Cu_3O_6$ mass fractions. Figure 5 shows that this expression fits all the data well with k_3 and k_4 values depending on carbon dioxide concentration. The parameters giving the best fit are reported in Table 1. The kinetic parameters fit closely ($R>$ 0.93) an Arrhenius temperature dependence. The corresponding values of the preexponential factors and activation energies are listed in Table 2. For the experiments at low carbon dioxide concentration (0.5 vol. %), the temperature impact is not consistent due to experimental scatter. While k_{30} and its activation energies are rather insensitive to changes in the CO_2 concentration, k_{40} and E_4 are very sensitive to changes in the CO_2 concentration.

Isothermal thermo-gravimetric experiments

Isothermal TG weight loss measurements were conducted to study the impact of operating conditions, sample size and fluid velocity on the rate of reaction 1 during the synthesis of $YBa_2Cu_3O_6$ from a precursor powder in the presence of different carbon dioxide concentrations in air. Most experiments were conducted using 20 mg samples, which completely filled the 2 mm high sample holders. The total gas-flow rate was 500 cm^3/min. This leads to a superficial gas velocity of 10 cm/s in the 3 cm^2 cross section of the TG.

The dependence of the weight loss due to the $BaCO_3$ decomposition at various CO_2 concentrations and the four different temperatures is shown in Figure 6. An initial weight loss of slightly more than 2%, which is independent of the carbon dioxide concentration is associated with the heating of the sample to the set temperature. The results indicate that high CO_2 partial pressures and low temperatures decrease the reaction rate and lower the final conversions of reaction 1. At 940°C, it takes 5 to 15 min to complete the reaction with increased CO_2 partial pressure, excluding 3% CO_2 at which the reaction is not completed even after 40 min. The reaction is completed after 15 to 40 min at 900°C, 50 to 100 min at 870°C, and 60 min to more than 4 h at 840°C. With 0.5% CO_2 it takes more than 40 min to complete the reaction at 870°C, 20 min at 900°C, and the reaction rate is almost instantaneous at 940°C. The experiments show that for each temperature a critical CO_2 concentration exists above which the rate of the weight loss is negligible. This critical CO_2 concentration increases with increasing temperature being 0.5 vol. % at 840°C and 4 vol. % at 940°C. The decomposition of these thick samples occurred at much higher temperatures (about 200°C) than those of the thin samples used in the XRD experiments.

The actual rate of the $BaCO_3$ decomposition and the final conversion were determined by subtracting the weight loss obtained for the critical CO_2 concentration from that obtained at lower CO_2 concentrations. Figure 7 describes the dependence of both the initial weight loss rate and the final conversion on the decomposition temperature and CO_2 concentrations. While the initial rate decreases smoothly with increasing CO_2 concentration, the final conversion drops rapidly as the CO_2 concentration exceeds some critical value, which increases with increasing temperature. This rapid conversion decrease is more pronounced at high temperatures.

Measurements of the weight loss at 760°C and different pure air flow rates reveal a decrease in the weight loss rate with decreasing air velocity (Figure 8a). In still air practically no weight loss due to $BaCO_3$ decomposition is observed. With a flow rate of 50 cm^3/min, the decomposition is slow (over 60 min) and not complete. With 250 to 500 cm^3/min most of the

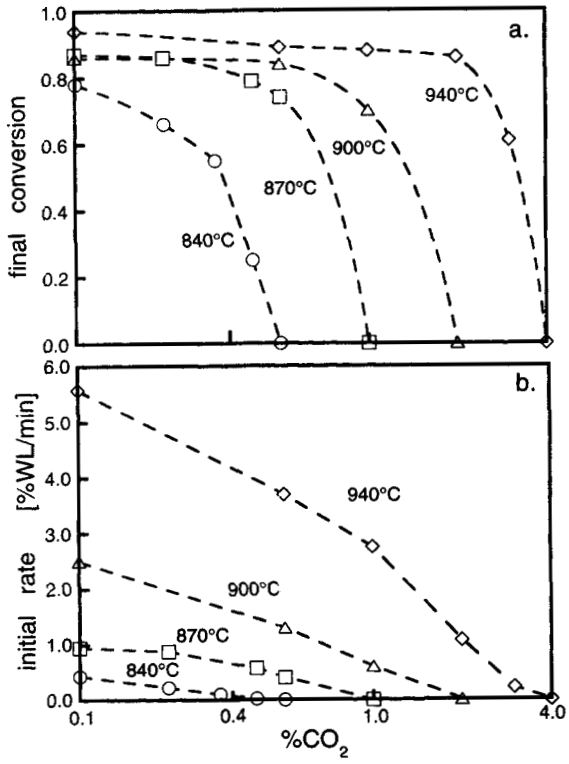

Figure 7. Effect of CO_2 partial pressure in air on the (a) final conversions; and (b) initial rates of the TG experiments.

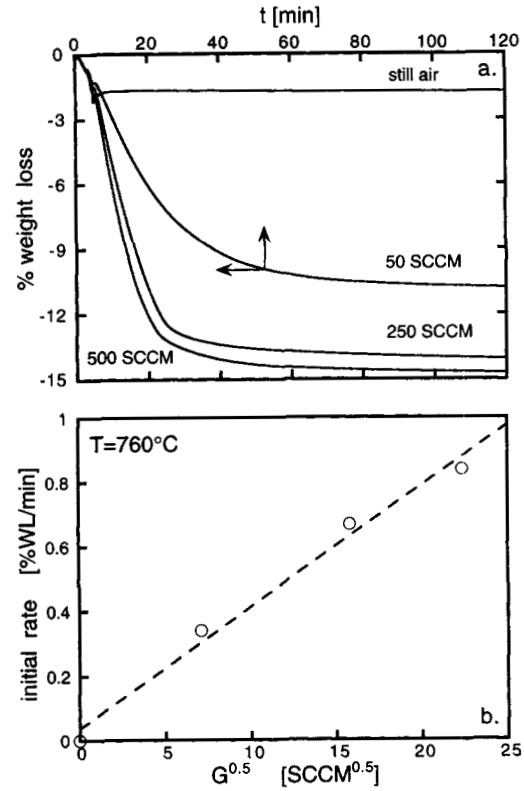

Figure 8. Effect of gas flow rate on the (a) TG weight loss; and (b) on the initial rates due to reaction 1 at 760°C and a 5 mg sample.

sample decomposes in less than 30 min. The experiments indicate that the carbon dioxide which evolves during the decomposition has a strong influence on the weight loss rate and can strongly inhibit the reaction rate if not removed by the flowing air from the system. The initial weight loss exhibits a linear dependence on the square root of the flow rate (Figure 8b). The laminar mass-transfer coefficient from a flat plate is proportional to the square of the Reynolds number. Thus, the square root dependence on the flow rate suggests that the rate of mass transfer from the sample to the flowing air has a strong impact on the observed rate and is a limiting step in the rate of $YBa_2Cu_3O_6$ synthesis. This mass-transfer coefficient is influenced by the shape and location of the sample holder in the furnace, the furnace dimension, and the location of the gas inlet and outlet. It is essential to account for the impact of the external transport-limitations in any attempt to determine the kinetics of the reaction or in the scale-up of the $YBa_2Cu_3O_6$ synthesis process.

Experiments using different amounts of precursor powder in the sample holder were carried out. Figure 9a shows the results at a temperature of 760°C and a flow rate of 500 cm^3/min. The experiments reveal that an increase in the sample weight, that is, height in the sample holder, decreases the reaction rate due to the evolved CO_2 in the sample voidage and pores. With 20 mg, it takes over 60 min for most of the decomposition to occur, with 10 mg it takes about 30 min, and less than 20 min with 5 mg. The initial rate depends linearly on the inverse mass, that is, the sample thickness (Figure 9b). The experiments indicate that removal of the evolved CO_2 from the sample limits the rate of $YBa_2Cu_3O_{7-x}$

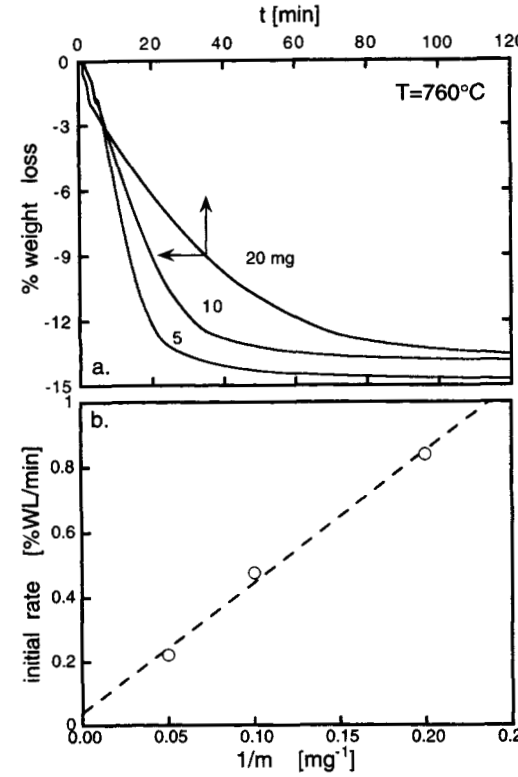

Figure 9. Effect of sample mass on (a) the TG weight loss; and (b) on the initial rates due to reaction 1 at 760°C and 500 cm^3/min gas-flow rate.

formation in thick samples. The observed reaction rate depends, in general, on the sample size, voidage, size distribution, and porosity of the precursor powder and the mass transfer to the ambient gas.

Discussion and Conclusions

The HT-XRD experiments show that increased CO_2 partial pressure shifts the $BaCO_3$ decomposition reaction (leading to $YBa_2Cu_3O_{7-x}$ formation) to higher temperatures and decreases the temperature range in which the reaction rate can be measured (with the time resolution of this instrument). At high (> 2%) CO_2 partial pressures, the reaction becomes essentially instantaneous with very high activation energy. Noninstantaneous nucleation of the reaction products delays the initiation of the reaction at low CO_2 partial pressures (0.5–1 vol. %) and temperatures (700°C).

In a thick sample (2 mm), the reactions occur in the 840 to 940°C range, which is about 200°C higher than that in a thin film (1 μm). In most HT-XRD experiments, the $BaCO_3$ decomposition was completed in less than 60 min, while in the TG experiments a high conversion was obtained only after several hours. The experiments showed that the rate of CO_2 diffusion within the sample pores and its transport to the ambient gas limited the rate of $BaCO_3$ decomposition in thick samples. The effectiveness factor and hence the observed reaction rate of a diffusion-limited catalytic or gas-liquid reaction is, in general, inversely proportional to the thickness of the sample. This strongly suggests that the linear dependence (weight loss) of the initial rate on 1/m (Figure 9b) is due to the interaction between the diffusion of the evolved CO_2 and the local reaction rate. We are currently attempting to determine the dependence of the intrinsic reaction rate on the local CO_2 concentration to enable development of models predicting the impact of the sample thickness on the reaction rate. The common practice of estimating the reaction rate from TG experiments may lead to severe pitfalls in the design of large-scale reactors, unless the samples are similar to the pellets used in the kiln.

Shelukar et al. (1994) calcined the same precursor powder we used in a continuous rotary kiln using a countercurrent gas-solid flow to enhance the CO_2 removal with solid and gas-flow rates of 10 to 40 g/h and 4 L/min, respectively. When the average solid residence time in the kiln was about 80 min (with 2.5% maximum CO_2 partial pressure in the gas phase), a nearly pure product was obtained. The solids spent about 25% of the residence time in the reaction zone, which was kept at a constant at 940°C. As a rough estimate then, formation within the kiln was complete in about 20 min, in agreement with the data presented here (Figure 6d). This suggests that while TG experiments produce strongly disguised kinetics that are quite different from the HT-XRD results, they are useful in explaining the range of temperatures and corresponding residence times for continuous rotary kiln calcination of $YBa_2Cu_3O_{7-x}$.

Our current understanding and ability to predict the rate of solid-solid reactions is very inferior to that of gaseous or liquid reactions. The combined use of HT-XRD and TG experiments provide a way of determining both the intrinsic kinetics and the impact of the transport limitations. This information is of both scientific interest and of practical value in the design of large-scale processes for synthesis of advanced ceramic materials.

Acknowledgments

This work was supported by the Texas Center for Superconductivity at the University of Houston under a grant from the State of Texas. We are thankful to SSC, Inc. for donating the precursor powder.

Literature Cited

Balachandran, U., S. L. Morissette, R. A. Russell, S. E. Dorris, and R. B. Poeppel, "Formation of Intermediate Compounds During Reduced Pressure Calcination of Y-Ba-Cu-O Precursor," *Proc. High Temp. Superconducting Compounds III: Processing and Microstructure Property Relationships*, S. H. Whang, A. DasGupta and E. Collins, eds. (1991).

Fawcett, T. G., C. E. Crowther, L. F. Whiting, J. C. Tou, W. F. Scott, R. A. Newman, W. C. Harris, F. J. Knoll, and V. J. Caldecourt, "The Rapid Simultaneous Measurement of Thermal and Structural Data by a Novel XRD/DSC Instrument," *Adv. in X-Ray Anal.*, **28**, 227 (1985).

Formica, J. P., K. M. Forster, J. T. Richardson, and D. Luss, "Kinetics of $YBa_2Cu_3O_6$ Formation Via *In Situ* XRD," *Superconductor Engineering AIChE Symp. Ser. 287*, T. O. Menash, ed., **88**, 1 (1992).

Forster, K. M., J. P. Formica, V. Milonopoulou, J. Kulik, J. T. Richardson, and D. Luss, "An *In Situ* Kinetic Study of $YBa_2Cu_3O_{7-x}$ Formation," *Proc. TcSUH Workshop on HTS Materials, Bulk Processing and Bulk Applications*, Houston, TX (1992).

Forster, K. M., J. P. Formica, J. T. Richardson, and D. Luss, "Solid-State Reaction Kinetics Determination via *In Situ* Time Resolved X-Ray Diffraction," *J. Solid State Chem.*, **108**, 152 (1994).

Gabriel, A., "Position Sensitive X-Ray Detector," *Rev. Sci. Instrum.*, **48**(10), 1303 (1977).

Gadalla, M. A., and T. Hegg, "Kinetics and Reaction Mechanisms for Formation and Decomposition of $YBa_2Cu_3O_x$, *Thermochim. Acta*, **145**, 149 (1989).

Garn, P. D., and O. Menis, "Certificate: ICTA Certified Reference Materials for Differential Thermal Analysis from 125–940°C," National Bureau of Standards, GPO, Washington, DC (1971).

Gerard, N., "Coupling of Thermogravimetric and X-Ray Diffraction Methods," *J. Phys. E.*, **7**, 509 (1974).

Grader, S. G., K. P. Gallagher, and A. D. Fleming, "Effect of Starting Particle Size and Vacuum Processing on the $YBa_2Cu_3O_x$ Phase Formation," *Chemistry of Mat.*, **1**, 665 (1989).

Hulbert, S. F., "Models for Solid State Reactions in Powdered Compacts: A Review," *J. Brit. Cer. Soc.*, **6**, 11 (1969).

Milonopoulou, V., K. M. Forster, J. P. Formica, J. Kulik, J. T. Richardson, and D. Luss, "Influence of Oxygen Partial Pressure on the Kinetics of $YBa_2Cu_3O_{7-x}$ Formation," *J. Mat. Res.*, **9**(2), 275 (1994).

Nix, R. M., T. Rayment, R. M. Lambert, J. R. Jennings, and J. Owen, "An In-Situ X-Ray Diffraction Study of the Activation and Performance of Methanol Synthesis Catalysts Derived from Rare Earth Copper Alloys," *J. of Cat.*, **106**, 216 (1987).

Poeppel, R. B., U. Balachandran, J. E. Emerson, S. A. Johnson, M. T. Lanagan, and C. A. Youngdahl, "Improved Processing of Ceramic Superconductors through Low Pressure Calcination," *Cer. Trans. Superconductivity and Cer. Superconductors*, K. M. Nair, ed., Amer. Cer. Soc., Westerville, OH (1990).

Ruckenstein, E., S. Narain, and N. Wu, "Reaction Pathways for the Formation of the $YBa_2Cu_3O_{7-x}$ Compound," *J. Mat. Res.*, **4**, 267 (1989).

SEIKO TG/DTA320 Operation Manual, Ver. 1, Seiko Instruments, (1989).

Shelukar, S. D., "Spray Roasting and Rotary Kiln Calcination for Synthesis of YBaCuO (123) Superconducting Powders," PhD Diss., Dept. of Chemical Engineering, Univ. of Houston, Houston, TX (1993).

Shelukar, S. D., H. G. K. Sundar, R. Semiat, J. T. Richardson, and D. Luss, "Continuous Rotary Kiln Calcination of YBaCuO Precursor Powders," *I&EC Res.*, **33**, 421 (1994).

Shie, S. H., and W. J. Thomson, "Low-Temperature Synthesis of $YBa_2Cu_3O_{7-x}$ Powders from Citrate and Nitrate Precursors," *Physica C*, **204**, 135 (1992).

Sinha, R. K., R. K. Sinha, and S. K. Srivastava, "Formation Behavior of $YBa_2Cu_3O_{7-x}$—Conventional Processing," *Supercond. Sci. Technol.*, **6**, 238 (1993).

Sundaresan, S., "Effect of Ambient Environment and Pressure on the Formation of $YBa_2Cu_3O_{6+x}$ from Y_2O_3, $BaCO_3$ and CuO," *Superconductor Engineering, AIChE Symp. Ser. 287*, T. O. Menash, ed., **88**, 1 (1992).

Thomson, J. W., K. A. Helling, and R. J. Rodriquez, "DXRD Studies of Oil Shale Mineral Reactions," *Energy & Fuels*, **2**, 9 (1988).

Thomson, J. W., H. Wang, B. D. Parkman, D. X. Li, M. Strasik, S. T. Luhman, C. Han, and A. I. Aksay, "Reactions Sequencing During Processing of the 123 Superconductor," *J. Amer. Ceram. Soc.*, **72**(10), 1977 (1989).

Walker, P. A., T. Rayment, and M. R. Lambert, "A Controlled Atmosphere *In Situ* X-Ray Diffraction Study of the Activation and Performance of Ammonia Synthesis Catalysts Derived from $CeRu_2$, $CeCO_2$, $CeFe_2$," *J. Cat.*, **117**, 102 (1989).

Wu, N. L., T. C. Wei, S. Y. Hou, and S. Y. Wong, "Kinetic Study and Modeling of the Solid-State Reaction $Y_2BaCuO_5 + 3BaCuO_2 + 2CuO \rightarrow 2YBa_2Cu_3O_{6.5-x} + xO_2$," *J. Mater. Res.*, **5**(10), 2056 (1990).

Manuscript received Oct. 2, 1996, and revision received Nov. 27, 1996.